Scattering of Electromagnetic Waves From Conducting Bernoulli Particles

BARIS ATES[1], ALP KUSTEPELI[2]
[1]Department of Mathematics,
Izmir Institute of Technology
Gulbahce Koyu Kampusu 35430, Urla, Izmir
TURKEY

[2]Department of Electrical & Electronics Engineering
Izmir Institute of Technology
Gulbahce Koyu Kampusu 35430, Urla, Izmir
TURKEY

Abstract: Scattering of electromagnetic plane waves from what we called Bernoulli particles is considered. These particles are obtained by the deformation of the sphere in radial direction via Bernoulli polynomials as smooth deformation functions. Analyses are carried out analytically by perturbation method. In order to achieve good accuracy, second order perturbation method is used. Present calculations enable to evaluate radar cross sections for arbitrary Bernoulli polynomials $B_n(\cos\theta)$. In the considered region, Bernoulli particles posses a noticeable property that there exists a correlation between the order of the polynomial and backward radar cross section.

Key-Words: Scattering, Radar Cross Section, Perturbation Method, Bernoulli Polynomials

Received: June 9, 2025. Revised: September 21, 2025. Accepted: December 23, 2025. Published: May 22, 2026.

1 Introduction

Analytical solution to the problem of scattering of electromagnetic plane waves from 3D obstacles is restricted for certain geometries, like sphere, infinite cylinder, spheroid and few others. The reason is that Helmholtz equation can be separated in only certain coordinate systems [1]. Thus, for a given arbitrarily shaped obstacle, one has to utilize approximation methods [2]

Perturbation method is quite similar to the Mie formulation because it uses the separation of variables and the assumption that the small deviations on the surface of obstacles lead to reasonable deviations on electromagnetic fields [3], [4], [5], [6], [7]. Thus, this method is mainly based on the expansion of the surface of the scatterers and the fields in terms of a smallness parameter. Boundary conditions on the surface of the scatterer enable to find the unknown coefficients of the perturbed fields. The accuracy of the method strongly depends on the order of the method, hence the second order method is applied in the present paper to attain more accurate results compared to the ones obtained by employing the first order theory.

Since perfectly shaped objects are rarely encountered in nature, nonspherical obstacles find a wide range application area in many different scientific disciplines. Among the various nonspherical obstacles, the Chebyshev particles, whose surfaces are obtained by the perturbation of the sphere with different Chebyshev polynomials $T_n(\cos\theta)$, may be the most famous ones that are commonly used to describe nonspherical rotationally symmetric obstacles [8]. However they are not sufficient to model all rotationally symmetric objects. Thus, describing new obstacle surfaces with new functions and obtaining their scattering properties are important to enhance our knowledge. Therefore, the aim of the present work is to extend the analysis of the nonspherical shapes by considering the novel family of the Bernoulli particles obtained by the deformation of the sphere by using the Bernoulli polynomials $B_n(\cos\theta)$ [9].

2 Formulation And Solution

Solution of Maxwell equations in spherical coordinates, under the assumption that time dependence is to be $e^{-i\omega t}$ with $i = \sqrt{-1}$, gives electric and magnetic fields by the followings [10]

$$\begin{aligned}
E_r &= \sum_{n,m} \frac{ia_{nm}}{\omega\mu\epsilon}\left(\frac{\partial^2}{\partial r^2}+k^2\right)(\,kr z_n(kr))P_n^m(\cos\theta)e^{im\varphi} \\
E_\theta &= \sum_{n,m} \frac{ia_{nm}}{\omega\mu\epsilon r}\frac{\partial}{\partial r}(kr\, z_n(kr))\frac{\partial}{\partial\theta}P_n^m(\cos\theta)e^{im\varphi} \\
&- \sum_{n,m} \frac{imb_{nm}}{\epsilon r\sin\theta}\; kr\, z_n(kr)P_n^m(\cos\theta)e^{im\varphi} \\
E_\varphi &= -\sum_{n,m} \frac{ma_{nm}}{\omega\mu\epsilon r\sin\theta}\frac{\partial}{\partial r}(kr\, z_n(kr))P_n^m(\cos\theta)e^{im\varphi} \\
&+ \sum_{n,m} \frac{b_{nm}}{\epsilon r} kr z_n(kr)\frac{\partial}{\partial\theta}P_n^m(\cos\theta)e^{im\varphi} \qquad (1)
\end{aligned}$$

where $\sum_{m,n} = \sum_{n=1}^{\infty}\sum_{m=-n}^{n}$, ω is the angular frequency, ϵ is the permittivity, μ is the permeability, and k is the wave number of the surrounding medium, $z_n(kr)$ are the spherical Bessel or Hankel functions, P_n^m is the associated Legendre function [9]. The coefficients a_{nm} and b_{nm} are arbitrary constants [11] and they are found by using the boundary conditions on the surface. Geometries considered in the present work are obtained from the sphere by deforming it in the radial direction as

$$r = r_s(\theta) = R\left(1 + \beta f_1(\theta) + \beta^2 f_2(\theta)\right) \quad (2)$$

where R is the radius of the reference sphere, β is the smallness parameter and the deformation functions seen in the equation are the Bernoulli polynomials and $f_1(\theta) = f_2(\theta) = B_n(\cos\theta)$. First few members of the Bernoulli polynomials are given below [9]:

$$B_0(\cos\theta) = 1 \quad (3)$$

$$B_1(\cos\theta) = \cos\theta - \frac{1}{2} \quad (4)$$

$$B_2(\cos\theta) = \cos^2\theta - \cos\theta + \frac{1}{6} \quad (5)$$

$$B_3(\cos\theta) = \cos^3\theta - \frac{3}{2}\cos^2\theta + \frac{1}{2}\cos\theta \quad (6)$$

$$B_4(\cos\theta) = \cos^4\theta - 2\cos^3\theta + \cos^2\theta - \frac{1}{30} \quad (7)$$

$$B_5(\cos\theta) = \cos^5\theta \quad (8)$$

For the geometries described by (2), unit normal vector is found to be

$$\begin{aligned}\hat{n} &= \left(1 - \beta^2\left(\frac{1}{2}(\frac{df_1}{d\theta})^2\right)\right)\hat{r} \\ &+ \left(-\beta\frac{df_1}{d\theta} + \beta^2 f_1\frac{df_1}{d\theta} - \beta^2\frac{df_2}{d\theta}\right)\hat{\theta} + O(\beta^3).\end{aligned}$$

Since the geometries have rotational symmetry, unit normal vector does not contain φ dependency. The related boundary conditions are

$$\hat{n}\times\vec{E}\big|_{r=r_s} = 0, \qquad \hat{n}.\vec{B}\big|_{r=r_s} = 0 \quad (9)$$

where $\vec{E}$ and $\vec{B}$ corresponds to the total electric and magnetic fields. By employing the perturbation method, they can be written in the form of

$$\vec{E}(r,\theta,\varphi) \;=\; \vec{E}_0 + \beta\vec{E}_1 + \beta^2\vec{E}_2 + O(\beta^3) \quad (10)$$

where $\vec{E}_0(r,\theta,\varphi)$ consists of two fields, the incident field and the scattered field from the sphere, and can be written as $\vec{E}_0(r,\theta,\varphi) = \vec{E}^{\text{inc}} + \vec{E}^{\text{sph}}$. Other terms $\vec{E}_1(r,\theta,\varphi)$ and $\vec{E}_2(r,\theta,\varphi)$ are the first and second order correction fields due to the perturbation of the surface. Since the boundary conditions (9) are enforced on the surface of the Bernoulli particles, by using Taylor expansions one can evaluate fields by considering $r_s = R + \Delta R$ where $\Delta R = \beta f_1 R + \beta^2 f_2 R$. The expressions for the field components up to the second order are obtained as:

$$\begin{aligned}E_{\gamma\alpha}(r_s,\theta,\varphi) &= E_{\gamma\alpha}(R+\Delta R,\theta,\varphi) \\ &= \Big[E_{\gamma\alpha}(r,\theta,\varphi) + \beta f_1 r\frac{\partial}{\partial r}E_{\gamma\alpha}(r,\theta,\varphi) \\ &+ \beta^2 f_2 r\frac{\partial}{\partial r}E_{\gamma\alpha}(r,\theta,\varphi) + \frac{\beta^2(f_1)^2 r^2}{2} \\ &\times \frac{\partial^2}{\partial r^2}E_{\gamma\alpha}(r,\theta,\varphi)\Big]_{r=R} + O(\beta^3) \quad (11)\end{aligned}$$

where α indicates the r, θ or φ component of the fields in spherical coordinates and γ denotes the order of fields $0, 1, 2$. Utilizing Taylor expansion, one can convert the boundary conditions evaluated on the surface of the deformed sphere to the system of equations evaluated on the sphere as:

$$\left[f_1 r\frac{\partial}{\partial r}E_{0\varphi} + E_{1\varphi}\right]_{r=R} = 0 \quad (12)$$

$$\left[-\frac{f_1^2 r^2}{2}\frac{\partial^2}{\partial r^2}E_{0\varphi} - f_1 r\frac{\partial}{\partial r}E_{1\varphi} - E_{2\varphi} - f_2 r\frac{\partial}{\partial r}E_{0\varphi}\right]_{r=R} = 0 \quad (13)$$

$$\left[f_1 r\frac{\partial}{\partial r}B_{0r} + B_{1r} - \frac{df_1}{d\theta}B_{0\theta}\right]_{r=R} = 0 \quad (14)$$

$$\begin{aligned}&\Big[\frac{f_1^2 r^2}{2}\frac{\partial^2}{\partial r^2}B_{0r} + f_1 r\frac{\partial}{\partial r}B_{1r} + B_{2r} - \frac{1}{2}\frac{d(f_1)^2}{d\theta}r\frac{\partial}{\partial r}B_{0\theta} \\ &-\frac{df_1}{d\theta}B_{1\theta} + \frac{1}{2}\frac{d(f_1)^2}{d\theta}B_{0\theta} + f_2 r\frac{\partial}{\partial r}B_{0r} - \frac{df_2}{d\theta}B_{0\theta}\Big]_{r=R} = 0. \quad (15)\end{aligned}$$

By the explicit expression of the fields in (1), one can evaluate the unknown coefficients a_{1nm}, b_{1nm} and a_{2nm}, b_{2nm} in terms of the coefficients a_{0nm} and b_{0nm} obtained from the solution of the sphere [12].

3 Scattering of Plane Waves From Deformed Conducting Sphere

In order to apply the perturbation method, firstly, the zeroth order solution belonging to the conducting sphere must be obtained. The incident field is a plane wave given in cartesian coordinates as $\vec{E}^{\text{inc}} = E^{\text{i}}e^{ikz}\hat{x}$ [11] and in spherical coordinates it takes take the following form [11];

$$\begin{aligned}\vec{E}^{\text{inc}}(r,\theta,\varphi) &= -iE^{\text{i}}\cos\varphi\sum_{n=0}^{\infty}\frac{i^n(2n+1)}{k_1 r}j_n(k_1 r)P_n^1(\cos\theta)\hat{r} \\ &+ E^{\text{i}}\cos\theta\cos\varphi\sum_{n=0}^{\infty}i^n(2n+1)j_n(k_1 r)P_n(\cos\theta)\hat{\theta} \\ &- E^{\text{i}}\sin\varphi\sum_{n=0}^{\infty}i^n(2n+1)j_n(k_1 r)P_n(\cos\theta)\hat{\varphi}.\end{aligned}$$

Since the total electric field consists of the summation of incident and scattered field, it is of the form $\vec{E} =$

$\vec{E}^{\text{inc}} + \vec{E}^{\text{s}}$. As mentioned above, the incident field can be written in the form of (1) and by using the boundary conditions in (9), one can find the zeroth order field coefficients a_{0nm} and b_{0nm} as [11] ;

$$a_{0nm} = \begin{cases} E^{\text{i}} \dfrac{i^n(2n+1)(kRj_n(kR))'}{2\omega n(n+1)(kRh_n^{(1)}(kR))'}, & m = 1 \\ -E^{\text{i}} \dfrac{i^n(2n+1)(kRj_n(kR))'}{2\omega(kRh_n^{(1)}(kR))'}, & m = -1 \\ 0 \quad , & m \neq \pm 1 \end{cases} \tag{16}$$

$$b_{0nm} = \begin{cases} E^{\text{i}} \dfrac{-i^{n+1}(2n+1)j_n(kR)}{2\omega\eta n(n+1)h_n^{(1)}(kR)}, & m = 1 \\ -E^{\text{i}} \dfrac{i^{n+1}(2n+1)j_n(kR)}{2\omega\eta h_n^{(1)}(kR)}, & m = -1 \\ 0 \quad , & m \neq \pm 1 \end{cases} \tag{17}$$

where the primes represent the derivatives with respect to the argument of the spherical Bessel and Hankel functions.

3.1 First Order Perturbed Fields

Since the zeroth order solution is known, one can now construct the perturbed fields. The total fields as mentioned are in the form,

$$\vec{E}(r,\theta,\varphi) = \vec{E}^{\text{inc}} + \vec{E}_0 + \beta\vec{E}_1 \tag{18}$$
$$\vec{B}(r,\theta,\varphi) = \vec{B}^{\text{inc}} + \vec{B}_0 + \beta\vec{B}_1. \tag{19}$$

The first order fields can be found by using the boundary condition (14) resulting to

$$B_{1r}(R,\theta,\varphi) = \Big[- f_1 r\frac{\partial}{\partial r}\Big(B_{0r}(r,\theta,\varphi) + B_r^{\text{inc}}(r,\theta,\varphi)\Big) + \frac{df_1}{d\theta}\Big(B_{0\theta}(r,\theta,\varphi) + B_\theta^{\text{inc}}(r,\theta,\varphi)\Big)\Big]_{r=R}. \tag{20}$$

Taking account of the field definitions, it would be convenient to write the deformation functions in terms of Legendre polynomials

$$f_1(\theta) = \sum_{j=0}^{\infty} f_j P_j(\cos\theta), \tag{21}$$

$$f_2(\theta) = \sum_{j=0}^{\infty} h_j P_j(\cos\theta), \tag{22}$$

$$\Big(f_1(\theta)\Big)^2 = \sum_{j=0}^{\infty} k_j P_j(\cos\theta). \tag{23}$$

Thus, multiplying both sides of (20) by $P_l^{m'}(\cos\theta)\sin\theta e^{-im'\varphi}$ and taking angular integrals gives b_{1nm} in terms of a_{0nm} and b_{0nm} [12]. To find the coefficients a_{1nm}, let us consider the following equation obtained from the boundary condition (12);

$$E_{1\varphi}(R,\theta,\varphi) = -\Big[f_1 r\frac{\partial}{\partial r}\Big(E_{0\varphi}(r,\theta,\varphi) + E_\varphi^{\text{inc}}(r,\theta,\varphi)\Big)\Big]_{r=R} \tag{24}$$

Multiplying both sides with $P_l^{m'}(\cos\theta)\sin^2\theta e^{-im'\varphi}$ and taking the angular integrals enables us to express the unknown coefficients a_{1nm} in terms of a_{0nm} and b_{0nm}.

3.2 Second Order Perturbed Fields

Since the zeroth and the first order fields are known, one can proceed to find the second order perturbed field which are expressed as

$$\vec{E}(r,\theta,\varphi) = \vec{E}^{\text{inc}} + \vec{E}_0 + \beta\vec{E}_1 + \beta^2\vec{E}_2 \tag{25}$$
$$\vec{B}(r,\theta,\varphi) = \vec{B}^{\text{inc}} + \vec{B}_0 + \beta\vec{B}_1 + \beta^2\vec{B}_2. \tag{26}$$

The boundary condition (15) is suitable to start with because it contains only the coefficients b_{2nm} as unknown;

$$B_{2r}(R,\theta,\varphi) = \Big[- \frac{f_1^2 r^2}{2}\frac{\partial^2}{\partial r^2}B_{0r} + \frac{1}{2}\frac{d(f_1)^2}{d\theta}\frac{r\partial}{\partial r}B_{0\theta} + \frac{df_1}{d\theta}B_{1\theta} - f_1 r\frac{\partial}{\partial r}B_{1r} - \frac{1}{2}\frac{d(f_1)^2}{d\theta}B_{0\theta} - f_2 r\frac{\partial}{\partial r}B_{0r} + \frac{df_2}{d\theta}B_{0\theta}\Big]_{r=R}. \tag{27}$$

Using the explicit expressions of the fields (1) and multiplication of the both sides of the above equality with the $P_l^{m'}(\cos\theta)\sin\theta e^{-im'\varphi}$ and integration allows one to obtain b_{2nm} [12]. To find the coefficients a_{2nm}, the following equation obtained from the boundary condition (13) can be used.

$$E_{2\varphi}(R,\theta,\varphi) = \Big[- \frac{f_1^2 r^2}{2}\frac{\partial^2}{\partial r^2}E_{0\varphi} - f_1 r\frac{\partial}{\partial r}E_{1\varphi} - f_2 r\frac{\partial}{\partial r}E_{0\varphi}\Big]_{r=R}. \tag{28}$$

Multiplication of the both sides with the $P_l^{m'}(\cos\theta)\sin^2\theta e^{-im'\varphi}$ and integration give a_{2nm}. With this result, we have completely found the unknown coefficients and determined the first and second order perturbed fields.

4 Validation and Numerical Results

In this section, analytically obtained results will be verified in terms of the radar cross section (RCS) [11]

$$\sigma = \lim_{r\to\infty}\left(4\pi r^2\frac{|\vec{E}^{\text{s}}|^2}{|\vec{E}^{\text{i}}|^2}\right). \tag{29}$$

According to the definition of total field in (10) the RCS results can be arranged in terms of the powers of the deformation parameter [6], [7]

$$\sigma = \sigma_0 + \beta\sigma_1 + \beta^2\sigma_2 + O(\beta^3) \tag{30}$$

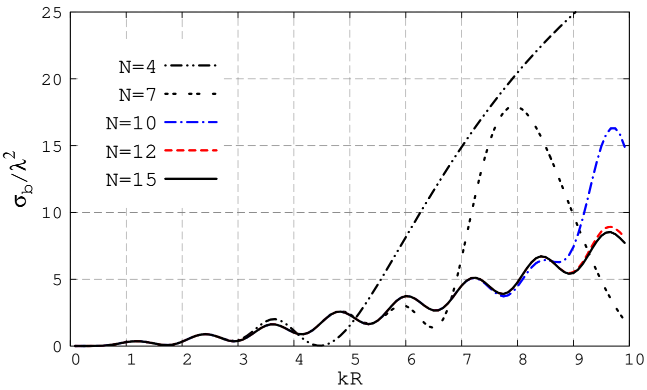

Fig. 1: Dependence of normalized backward radar cross section result on maximum summation term N.

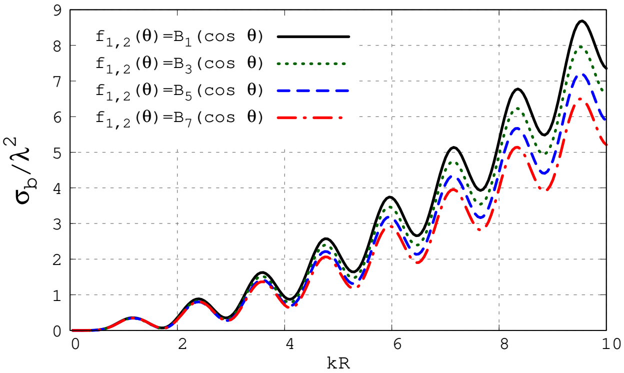

Fig. 2: Backward RCS of the odd Bernoulli particles when maximum deviation $\Delta_0 = 0.3$.

where σ_0 corresponds to RCS from the sphere, σ_1 and σ_2 are the first and the second order corrections, respectively. This representation is quite useful and makes perturbation method indispensable in RCS calculations. Since σ_0, σ_1, and σ_2 are independent of β, once they have been obtained for a geometry, they can be repeatedly used to evaluate RCS results for different deformation parameters. In this sense, the representation (30) can be regarded as size and shape effect factorized representation of the RCS.

In order to evaluate radar cross section (29), infinite summations of the fields in (1) must be truncated at a finite number $n = N$ such that resulting expression to be within the desired accuracy. Since we deal with deformed spheres, it would be convenient to see the effect of truncation number on the accuracy by taking targets as spheres namely in Mie Theory. From Figure 1, it can be seen that truncation number $N = 15$ is sufficient.

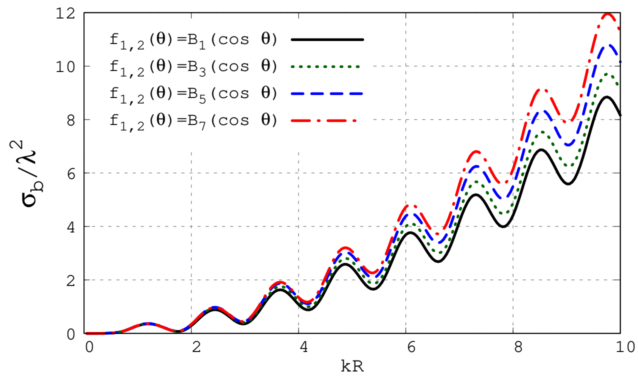

Fig. 3: Backward RCS of the odd Bernoulli particles when maximum deviation $\Delta_0 = -0.3$.

We can now proceed to find and discuss the RCS results of Bernoulli particles which are obtained by the deformation of sphere with deformation function in the form of Bernoulli polynomials. Bernoulli polynomials, unlike the Chebyshev polynomials, do not take the values between -1 and 1. They can take larger values depending on the order of the polynomial. This situation enforced us to follow a different recipe in order to guarantee not to exceed the limits of the perturbation method and to stay within the range of applicability. Since the deformation of the sphere is of the form $r_s = R + \Delta R$ with

$$\Delta R = (\beta + \beta^2) B_n(\cos\theta) R, \tag{31}$$

in order to compare the effect of different deformation functions, we first fix the amount of deviation, say $\Delta R = \Delta_0$, then we solve the equation (31) for β which guarantees the maximum deviation Δ_0.

For the comparison purposes, the radius R and the maximum deviation Δ_0 are chosen as $R = 10$ and $\Delta_0 = 0.3$, the odd Bernoulli polynomials taken into consideration vary from $B_1(\cos\theta)$ up to $B_7(\cos\theta)$ and the resulting deformation parameters are obtained from (31) as mentioned. As it can be seen from Figure 2, for this fixed deviation, when the degree of the polynomial increases, the backward RCS result decreases in almost whole considered region.

In Figure 3, backward RCS results are again presented for the same Bernoulli particles used in Figure 2 but the maximum deviation to be $\Delta_0 = -0.3$ by choosing the deformation parameters in (31) accordingly. As can be seen from Figure 3, for this fixed deviation, if the degree of the polynomial increases, the backward RCS result increases in almost whole considered region. The behaviors of the RCS results seen in the previous figures for $\Delta_0 = \pm 0.3$ have been observed when $\Delta_0 = \pm 0.1$ and $\Delta_0 = \pm 0.2$ as well.

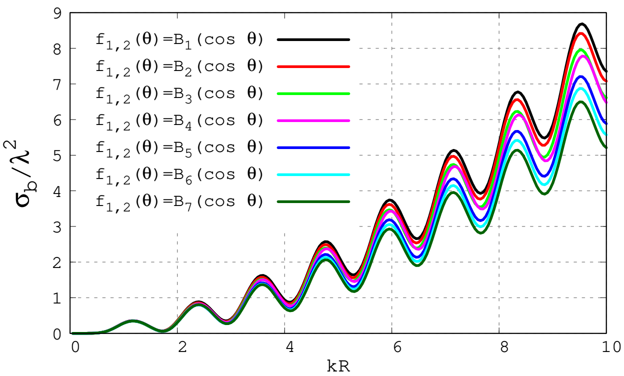

Fig. 4: Backward RCS for some Bernoulli particles when the maximum deviation $\Delta_0 = 0.3$.

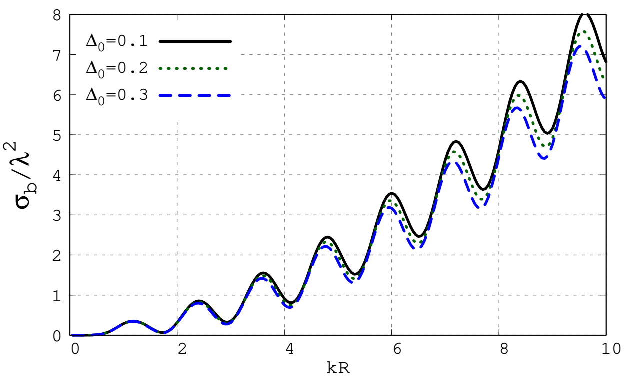

Fig. 5: Backward RCS for the fixed deformation function $f_1 = f_2 = B_5(\cos\theta)$ with different positive deviations.

Gathering all of the information mentioned above, it can be concluded that both the amount and the sign of the maximum deviation are important for RCS results.

The backward RCS sequential results from $B_1(\cos\theta)$ up to $B_7(\cos\theta)$ for $\Delta_0 = 0.3$ are shown in Figure 4. As it can be seen the RCS results are ordered according to the order of Bernoulli polynomials. In Figure 5, in order to analyze the effect of deformation parameter, backward RCS results for fixed deformation function with different deformation parameters and hence for different maximum deviations are considered. It is seen from the figure that, for the deformation function $B_5(\cos\theta)$, among the positive deviations the highest RCS result belongs to the deviation $\Delta_0 = 0.1$. It can also be seen in Figure 5 when the maximum positive deviation Δ_0 increases, the RCS result decreases.

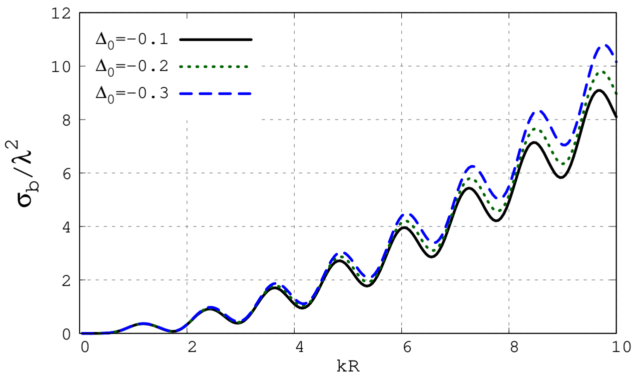

Fig. 6: Backward RCS for the fixed deformation function $f_1 = f_2 = B_5(\cos\theta)$ with different negative deviations.

In Figure 6, negative deviations are considered and as shown in the figure increasing the amount of the inward deviations causes an increment on the RCS results in almost whole considered interval. Thus, the biggest RCS result is obtained for $\Delta_0 = -0.3$. By analyzing the above results, one may conclude that these new nonspherical particles possess quite important scattering properties and for fixed deviations there exist a correlation between the order of the Bernoulli polynomials and radar cross section results.

5 Conclusion

In the present work scattering of electromagnetic plane waves from conducting Bernoulli particles were considered. These particles were obtained from the deformation of conducting sphere in radial direction with small deformation parameters and Bernoulli polynomials as deformation functions. These particles have rotational symmetry like other important ones such as spheroidal particles, Chebyshev particles and other ones whose shapes are in the form of body of revolution. These new particles possess interesting scattering features that systematic correlations between the order of Bernoulli polynomials and radar cross section were observed.

References:

[1] P. M. Morse and H. Feshbach, Methods of Theoretical Physics, *McGraw - Hill Science*, 1953.

[2] M. I. Mishchenko, “T-matrix theory of electromagnetic scattering by particles and its applications: a comprehensive

reference database," *J. Quant. Spect. Rad. Trans.*, vol. 88, pp. 357-406, 2004, doi:10.1016/j.jqsrt.2004.05.002.

[3] V. A. Erma, "Exact solution for the scattering of electromagnetic waves from conductors of arbitrary shape, II, general case," *Phys. Rev.*, vol. 176, no. 5, 1968, https://doi.org/10.1103/PhysRev.173.1243.

[4] U. Raval and C. P. Gupta, "Electromagnetic scattering due to the deformed inhomogeneous bodies part1 sphere," *Pure and Appl. Geophys.*, vol. 87, no. 1, pp. 134-145, 1971, https://doi.org/10.1007/BF00878917.

[5] C. Yeh, "Perturbation approach to the diffraction of electromagnetic waves by arbitrarily shaped dielectric obstacles," *Phys. Rev.*, vol. 135, no. 5A, pp. 1193-1201, 1964, https://doi.org/10.1103/PhysRev.135.A1193.

[6] A. D. Kotsis and J. A. Roumeliotis, "Electromagnetic scattering by a metallic spheroid using shape perturbation method," *PIER.*, vol. 67, pp. 113-134, 2007, doi:10.2528/PIER06080202.

[7] G. P. Zouros, A. D. Kotsis and J. A. Roumeliotis, "Electromagnetic scattering from a metallic prolate or oblate spheroid using asymptotic expansions on spheroidal eigenvectors," *IEEE Trans. on Antennas and Propagat.*, vol. 62, no. 2, pp. 839-851, 2014, doi:10.1109/TAP.2013.2289363.

[8] A. Mugnai and W. J. Wiscombe, Scattering from nonspherical Chebyshev particles. I: cross sections, single-scattering albedo, asymmetry factor, and backscattered fraction. *Applied optics*, vol. 25, no.7, pp. 1235-1244, 1986, https://doi.org/10.1364/AO.25.001235.

[9] G. B. Arfken and H. J. Weber, Mathematical Methods for Physicist. California, USA: *Elsevier Academic Press*, 2015.

[10] H. J. Eom, Electromagnetic Wave Theory for Boundary Value Problems, an Advanced Course on Analytical Methods. Berlin, Germany: *Springer-Verlag*, 2004.

[11] C. A. Balanis, Advanced Engineering Electromagnetics. Newyork, NY, USA: *John Wiley & Sons*, 1989.

[12] B. Ates, A. Kustepeli, and Z. Cetin, Analytical improvement on the electromagnetic scattering from deformed spherical conducting objects. *IEEE Transactions on Antennas and Propagation*, vol. 69, no.12, pp. 8630-8640, 2021, doi:10.1109/TAP.2021.3096317.

Contribution of Individual Authors to the Creation of a Scientific Article (Ghostwriting Policy)

The authors equally contributed in the present research, at all stages from the formulation of the problem to the final findings and solution.

Sources of Funding for Research Presented in a Scientific Article or Scientific Article Itself

No funding was received for conducting this study.

Conflicts of Interest

The authors have no conflicts of interest to declare that are relevant to the content of this article.